Article

Mechanistic Investigation of the Staudinger Ligation

Fiona L. Lin, Helen M. Hoyt, Herman van Halbeek, Robert G. Bergman, and Carolyn R. Bertozzi

J. Am. Chem. Soc., **2005**, 127 (8), 2686-2695• DOI: 10.1021/ja044461m • Publication Date (Web): 01 February 2005

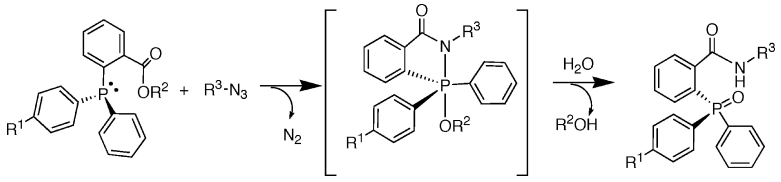

More About This Article

Additional resources and features associated with this article are available within the HTML version:

- Supporting Information
- Links to the 27 articles that cite this article, as of the time of this article download
- Access to high resolution figures
- Links to articles and content related to this article
- Copyright permission to reproduce figures and/or text from this article

View the Full Text HTML

J|A|C|S
ARTICLES
Published on Web 02/01/2005

Mechanistic Investigation of the Staudinger Ligation

Fiona L. Lin,[†] Helen M. Hoyt,[†] Herman van Halbeek,[†] Robert G. Bergman,[†] and Carolyn R. Bertozzi*[,†,‡,§,¶]

Contribution from the Departments of Chemistry and Molecular and Cell Biology and Howard Hughes Medical Institute, University of California, and Materials Sciences Division, Lawrence Berkeley National Laboratory, Berkeley, California 94720

Received September 13, 2004; E-mail: crb@berkeley.edu

Abstract: The Staudinger ligation of azides and phosphines has found widespread use in the field of chemical biology, but the mechanism of the transformation has not been characterized in detail. In this work, we undertook a mechanistic study of the Staudinger ligation with a focus on factors that affect reaction kinetics and on the identification of intermediates. The Staudinger ligation with alkyl azides was second-order overall and proceeded more rapidly in polar, protic solvents. Hammett analyses demonstrated that electron-donating substituents on the phosphine accelerate the overall reaction. The electronic and steric properties of the ester had no significant impact on the overall rate but did affect product ratios. Finally, the structure of an intermediate that accumulates under anhydrous conditions was identified. These findings establish a platform for optimizing the Staudinger ligation for expanded use in biological applications.

Introduction

Bioorthogonal chemical reactions, in which the coupling partners react selectively without interference by biological functionality, have become important tools in the field of chemical biology.[1] As an example, the Staudinger ligation of azides and arylphosphines[2,3] (Scheme 1) results in selective formation of an amide bond within complex biological environs, such as cells[4] and living animals.[5] This reaction has been employed in a wide range of applications, including modification of cell surfaces,[2,4] protein engineering,[6,7] specific labeling of nucleic acids,[8] proteomic studies,[9,10] and as a general tool for bioconjugation.[11,12]

While appreciation of the Staudinger ligation as a tool for chemical biology continues to expand, little attention had been directed to fundamental mechanistic studies that would allow for optimization of rates and yields. Herein, we report the first mechanistic investigation of the Staudinger ligation, including the determination of kinetic parameters and solvent effects, Hammett analyses of substituent effects, and the structural elucidation of a reaction intermediate.

Scheme 1

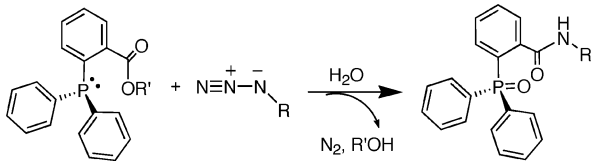

Results and Discussion

Investigation of the Kinetic Parameters of the Staudinger Ligation by ^{31}P NMR Spectroscopy. The Staudinger ligation is a modified version of the classical Staudinger reaction[13] between phosphines and azides. Mechanistic studies of the classical reaction between triphenylphosphine (**1**, R = Ph) and phenyl azide (**2**, R′ = Ph) suggest that the lone pair electrons of **1** attack the terminal nitrogen atom of the azide (**2**) to yield a linear phosphazide intermediate **3** (Scheme 2).[14−18] This intermediate can undergo intramolecular rearrangement via a four-membered ring transition state to yield a second intermediate, azaylide **4** (also known as an iminophosphorane), with concomitant loss of N_2. In the presence of water, azaylide **4** undergoes hydrolysis to yield amine **5** and phosphine oxide **6**.

[†] Department of Chemistry.
[‡] Department of Molecular and Cell Biology.
[§] Howard Hughes Medical Institute.
[¶] Lawrence Berkeley National Laboratory.

(1) Hang, H. C.; Bertozzi, C. R. *Acc. Chem. Res.* **2001**, *34*, 727−736.
(2) Saxon, E.; Bertozzi, C. R. *Science* **2000**, *287*, 2007−2010.
(3) Kohn, M.; Breinbauer, R. *Angew. Chem., Int. Ed.* **2004**, *43*, 3106−3116.
(4) Saxon, E.; Luchansky, S. J.; Hang, H. C.; Yu, C.; Lee, S. C.; Bertozzi, C. R. *J. Am. Chem. Soc.* **2002**, *124*, 14893−14902.
(5) Prescher, J. A.; Dube, D. H.; Bertozzi, C. R. *Nature* **2004**, *430*, 873−877.
(6) Nilsson, B. L.; Hondal, R. J.; Soellner, M. B.; Raines, R. T. *J. Am. Chem. Soc.* **2003**, *125*, 5268−5269.
(7) Kiick, K. L.; Saxon, E.; Tirrell, D. A.; Bertozzi, C. R. *Proc. Natl. Acad. Sci. U.S.A.* **2002**, *99*, 19−24.
(8) Wang, C. C.-Y.; Seo, T. S.; Li, Z.; Ruparel, H.; Ju, J. *Bioconjugate Chem.* **2003**, *14*, 697−701.
(9) Hang, H. C.; Yu, C.; Kato, D. L.; Bertozzi, C. R. *Proc. Natl. Acad. Sci. U.S.A.* **2003**, *100*, 14846−14851.
(10) Vocadlo, D. J.; Hang, H. C.; Kim, E. J.; Hanover, J. A.; Bertozzi, C. R. *Proc. Natl. Acad. Sci. U.S.A.* **2003**, *100*, 9116−9121.
(11) Soellner, M. B.; Dickson, K. A.; Nilsson, B. L.; Raines, R. T. *J. Am. Chem. Soc.* **2003**, *125*, 11790−11791.
(12) Kohn, M.; Wacker, R.; Peters, C.; Schroder, H.; Soulere, L.; Breinbauer, R.; Niemeyer, C. M.; Waldmann, H. *Angew. Chem., Int. Ed.* **2003**, *42*, 5830−5834.
(13) Staudinger, H.; Meyer, J. *Helv. Chim. Acta* **1919**, *2*, 635−646.
(14) Gololobov, Y. G.; Zhmurova, I. N.; Kasukhin, L. F. *Tetrahedron* **1981**, *37*, 437−472.
(15) Gololobov, Y. G.; Kasukhin, L. F. *Tetrahedron* **1992**, *48*, 1353−1406.
(16) Johnson, A. W. *Ylides and Imines of Phosphorus*; Wiley: New York, 1993.
(17) Leffler, J. E.; Tsuno, Y. *J. Org. Chem.* **1963**, *28*, 902−906.
(18) Leffler, J. E.; Temple, R. D. *J. Am. Chem. Soc.* **1967**, *89*, 5235−5246.

10.1021/ja044461m CCC: $30.25

Scheme 2

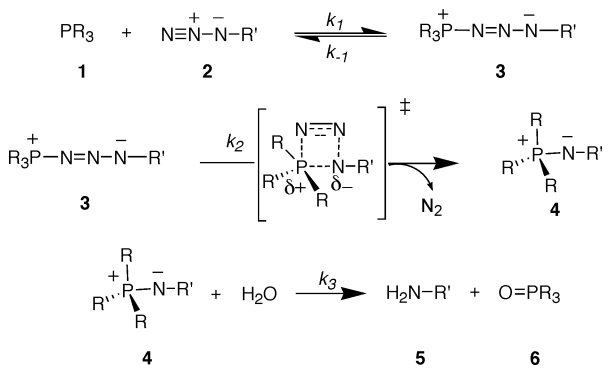

Scheme 3

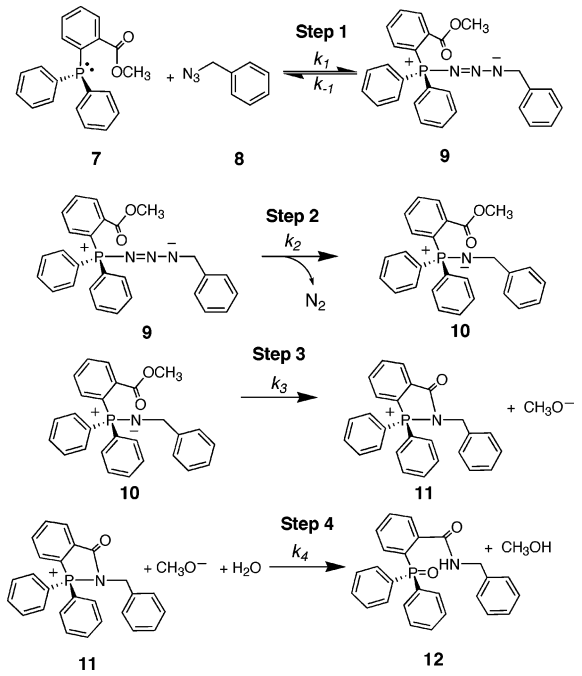

Scheme 3 depicts a typical Staudinger ligation between phosphine **7** and benzyl azide (**8**) to yield azaylide **10**. We presume that the early steps of the Staudinger ligation (steps 1 and 2, Scheme 3) are similar to those of the classical reaction. The major difference between the Staudinger ligation and the classical reaction is that azaylide **10** can undergo an intramolecular reaction (step 3) to produce a new intermediate, for which we previously proposed structure **11**.[2] Finally, the intermediate undergoes hydrolysis to afford amide-linked product **12** (step 4).

Kinetic studies of the classical Staudinger reaction have shown that the process can be first- or second-order overall depending on the exact nature of the reactants. For example, the rate-limiting step in the reaction between triphenylphosphine (**1**, Scheme 2, R = Ph) and benzenesulfonyl azide (**2**, R′ = $PhSO_2$) is the unimolecular decomposition (k_2, Scheme 2) of the phosphazide complex.[17] In contrast, the reaction of benzoyl azide (**2**, R′ = PhCO) and triphenylphosphine follows second-order kinetics, indicating that the bimolecular step leading to the formation of the phosphazide (k_1, Scheme 2) is rate-limiting.[18] In reactions between substituted phenyl azides and substituted triphenylphosphines, deviations from second-order kinetics are observed, presumably due to the reversibility of formation of the phosphazide intermediate (k_{-1}, Scheme 2).[18]

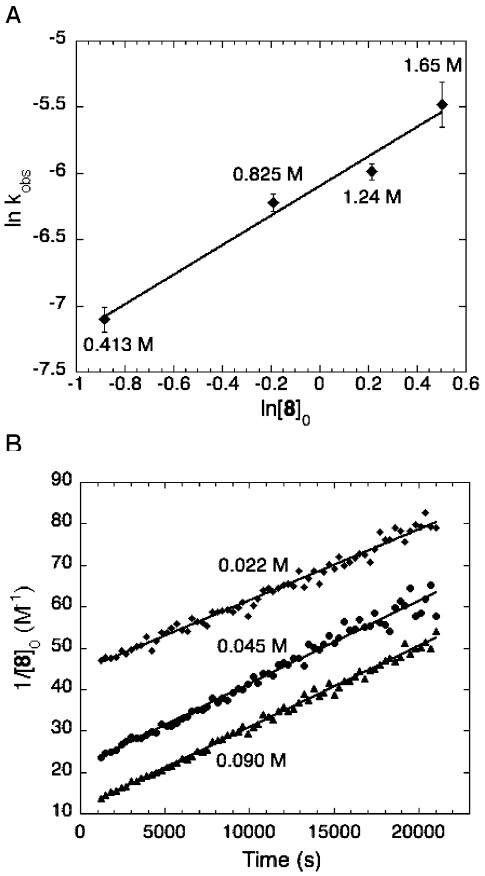

Figure 1. Kinetic analysis of the Staudinger ligation of phosphine **7** and benzyl azide (**8**). (A) Plot of ln k_{obs} versus ln [**8**]$_0$ to determine the second-order rate constant under pseudo-first-order conditions, where **8** was used in excess. Pseudo-first-order rate constants were measured at [**7**] = 0.041 M and [H_2O] = 2.8 M in CD_3CN at 20−21 °C. The second-order rate constant is calculated to be $(2.5 \pm 0.2) \times 10^{-3}$ M^{-1} s^{-1} from the *y*-intercept of the least-squares fit, with an estimated 10% error. (B) Plot of 1/[**8**]$_0$ versus time to determine the second-order rate constant of the Staudinger ligation between phosphine **7** and benzyl azide (**8**) under stoichiometric conditions in CD_3CN with 5% (v/v) H_2O. The slopes of the linear fits represent the second-order rate constants according to the kinetic model for a second-order reaction. At each concentration of substrate, linear fits were obtained with similar slopes of approximately 2×10^{-3} M^{-1} s^{-1}.

We determined the kinetic parameters of the Staudinger ligation of phosphine **7** and benzyl azide (**8**) (Scheme 3) using ^{31}P NMR spectroscopy. When **7** (0.041 M) and **8** (0.41 M) were combined in CD_3CN with 5% water (v/v) (2.78 M), consumption of **7** followed pseudo-first-order kinetics. Under these conditions, the only species detectable by ^{31}P NMR were the starting material **7** and the ligation product **12**. The pseudo-first-order rate constants, k_{obs}, for the consumption of **7** using different concentrations of excess benzyl azide (0.41, 0.82, 1.24, and 1.65 M) were measured and used to determine the second-order rate constant (k_1, Scheme 3). By plotting ln k_{obs} versus ln [**8**]$_0$, the overall second-order rate constant was determined to be $(2.5 \pm 0.2) \times 10^{-3}$ M^{-1} s^{-1} (Figure 1A). Consistent with that of the mechanism of the classical Staudinger reaction, the rate-limiting step of the Staudinger ligation is presumably the initial reaction between **7** and **8** to yield phosphazide **9** (k_1, Scheme 3). Since no intermediates were detected and the observed kinetics were in good agreement with a kinetic model for bimolecular reactions, this first step is likely to be irreversible.

Table 1. Pseudo-First-Order Rate Constants of the Staudinger Ligation of Phosphine **7** (0.044 M) and Benzyl Azide (0.83 M) in Different Solvents[a]

solvent	ϵ[b]	k_{obs} (10^{-3} $M^{-1}s^{-1}$) 2.5% H_2O (v/v) (1.39 M)	k_{obs} (10^{-3} $M^{-1}s^{-1}$) 5% H_2O (v/v) (2.78 M)	k_{obs} (10^{-3} $M^{-1}s^{-1}$) 10% H_2O (v/v) (5.56 M)
THF-d_8	7.6	0.83 ± 0.02	0.93 ± 0.03	1.4 ± 0.3
Acetone-d_6	20.7	1.3 ± 0.2	1.2 ± 0.2	1.44 ± 0.01
CD_3OD	32.7	2.6 ± 0.5	3.8 ± 0.1	3.6 ± 0.7
CD_3CN	37.5	1.9 ± 0.1	1.9 ± 0.2	2.4 ± 0.2
DMSO-d_6	46.7	2.06 ± 0.04	2.92 ± 0.08	3.6 ± 0.5

[a] Reported rate constants represent the average of three runs under each condition ±5% standard deviation. [b] From: Riddick, J. A.; Bunger, W. B. Organic Solvents. In *Techniques of Chemistry*; Weissberger, A., Ed.; Wiley: New York, 1970; Vol. II.

To ensure that the Staudinger ligation behaves similarly under stoichiometric conditions, the kinetics of the reaction using equimolar amounts of both reactants and excess water were also investigated. Under these conditions, the observed kinetics were consistent with a second-order reaction characterized by a rate constant of $(1.9 \pm 0.1) \times 10^{-3}$ M^{-1} s^{-1} (Figure 1B). This rate constant is in good agreement with that obtained under pseudo-first-order conditions, indicating that the reaction behaves similarly at different substrate concentrations.

Effects of Changes in Solvent Polarity on Staudinger Ligation Rates. Using a series of organic solvents that are miscible with water, we investigated the effect of changes in solvent polarity on the rate of the Staudinger ligation. The results are summarized in Table 1. In general, the reaction proceeded faster in solvents with higher dielectric constants. These observations indicate that the rate-limiting step involves a polar transition state that can be stabilized by polar solvents. Furthermore, the sensitivity of the observed rate constants to different concentrations of water varied in different solvents. For example, the rate constants observed in the presence of 1.39, 2.78, and 5.56 M water in acetone-d_6 were similar, but in DMSO-d_6, the rate constants varied more significantly. It is also interesting to note that the observed rate constants for reactions performed in CD_3OD are significantly higher than those in CD_3CN, even though the two solvents have very similar dielectric constants. These observations suggest additional contributions of the solvent to transition state stabilization through hydrogen bonding or other direct interactions.

Effects of Phosphine Substituents on Staudinger Ligation Rates. Three panels of phosphines were synthesized in order to determine the effects of steric and electronic modifications on the overall reaction (Figure 2). In series A, the steric bulk of the ester was varied. Phosphines **13a**−**d** were treated with benzyl azide in CD_3CN with 5% water (v/v), and the products and pseudo-first-order rate constants were characterized (Table 2). The size of the leaving group did not have a significant effect on the overall rate, indicating that ester cleavage is not involved in the rate-limiting step. Interestingly, in the reactions of phosphines with relatively small leaving groups (R = Me, Et, and *i*-Pr), only the Staudinger ligation product was observed. However, when the leaving group was more sterically demanding (R = *t*-Bu), a significant amount of the phosphine oxide derived from direct hydrolysis of the azaylide intermediate was also observed (shown schematically in Table 2). This observation is consistent with a mechanism in which the rate-limiting step is the bimolecular formation of the phosphazide (step 1, Scheme 3), whereas the ligation:hydrolysis product ratio is governed by the rate of intramolecular amide formation (step 3) versus hydrolysis of the azaylide. Thus, better ligation yields should be expected with relatively small ester leaving groups.

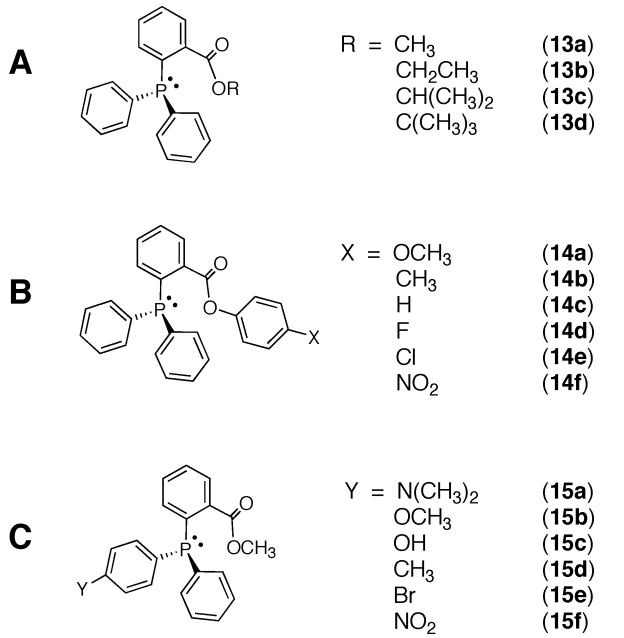

Figure 2. Phosphines synthesized to investigate the effects of steric and electronic modifications on the rate of the Staudinger ligation.

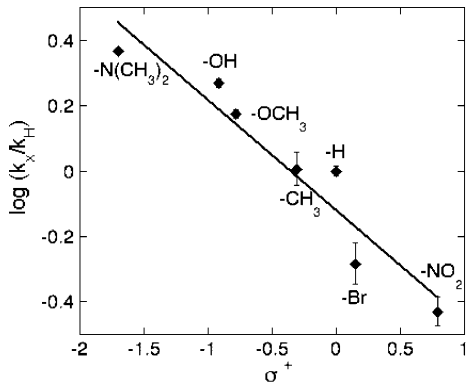

Figure 3. Hammett analysis for substituents on the phenyl group directly attached to the phosphorus center. Reactions were performed with phosphines **15a**−**f** (0.020 M) and benzyl azide (**8**) (0.83 M) in 5% (v/v) H_2O in CD_3CN at room temperature.

On the basis of the above results, one would not expect the electronic properties of the ester leaving group to affect the overall rate of the reaction. To test this hypothesis, we prepared phosphines **14a**−**f** (Figure 2, series B) functionalized with a series of para-substituted phenol esters. The observed pseudo-first-order rate constants were indeed very similar (Table 3). Taken together, these results support a mechanism in which the

Table 2. Pseudo-First-Order Rate Constants and Product Distribution for the Staudinger Ligation of Phosphines **13a**−**d** and Benzyl Azide in CD_3CN with 5% (v/v) H_2O[a]

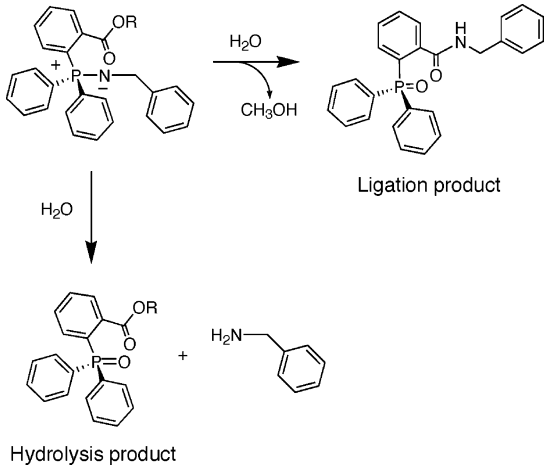

phosphine	R	LP:HP[b]	k_{obs} (10^{-3} M^{-1} s^{-1})
13a	CH_3	100:0	2.0 ± 0.1
13b	CH_2CH_3	100:0	1.9 ± 0.1
13c	$CH(CH_3)_2$	100:0	2.0 ± 0.2
13d	$C(CH_3)_3$	60:40	1.8 ± 0.3

[a] Reported rate constants represent the average of three runs under each condition ±5% standard deviation. [b] LP = ligation product; HP = hydrolysis product. Product ratios determined by ^{31}P NMR peak integrations.

Table 3. Pseudo-First-Order Rate Constants of the Staudinger Ligation of Phosphines **14a**−**f** and Benzyl Azide in CD_3CN with 5% (v/v) H_2O[a]

phosphine	X	σ_{para}[b]	k_{obs} (10^{-3} M^{-1} s^{-1})
14a	OCH_3	−0.27	2.0 ± 0.2
14b	CH_3	−0.17	2.0 ± 0.2
14c	H	0	1.8 ± 0.2
14d	F	0.06	1.9 ± 0
14e	Cl	0.23	2.2 ± 0.1
14f	NO_2	0.78	1.9 ± 0.4

[a] Reported rate constants represent the average of three runs under each condition ±5% standard deviation. [b] Values are those given by Ritche, C. D.; Sager, W. F. *Prog. Phys. Org. Chem.* **1964**, *2*, 323.

rate-limiting step occurs prior to intramolecular reaction of the azaylide group with the ester functionality.

Unlike substituents on the ester leaving group, substituents on a phenyl group directly attached to the phosphorus atom (Figure 2, series C, **15a**−**f**) had a pronounced effect on the overall rate. Figure 3 shows the Hammett plot of log (k_x/k_H) versus the σ^+ values of the substituents. A linear fit ($R^2 = 0.91$) with a small ρ value (−0.38) was obtained. The negative ρ value suggests a buildup of positive charge in the rate-limiting transition state, consistent with formation of the phosphazide (step 1, Scheme 3) as the rate-determining step. From a practical standpoint, these results suggest that the overall rate of the Staudinger ligation can be accelerated by electron-donating substituents on the phosphine. Indeed, in the future, we plan to investigate the reactivity of triarylphosphines with electron-donating substituents on each phenyl group.

Effects of Azide Structure on Staudinger Ligation Rates. We further probed the kinetic parameters of the Staudinger ligation as a function of azide structure. Three aryl azides (**16a**−**c**, Scheme 4) were prepared and treated with phosphine **7** using conditions previously applied with benzyl azide (0.041

Scheme 4

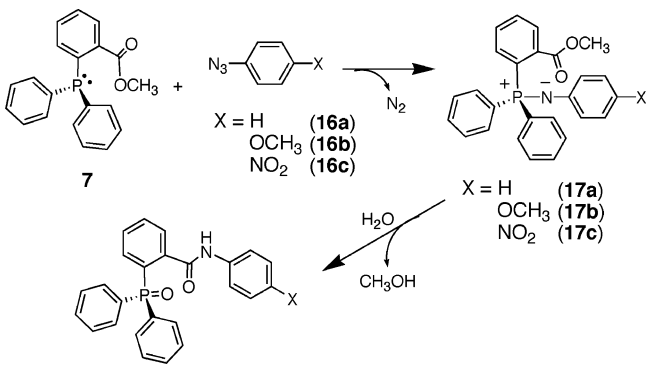

M phosphine and 0.41 M azide in CD_3CN with 5% water (v/v)). The products and reaction rates were determined using ^{31}P NMR spectroscopy. The reaction with phenyl azide (**16a**) as a substrate proceeded rapidly to produce a stable intermediate with a ^{31}P resonance at ca. +13 ppm. This intermediate was proposed to be azaylide **17a**, consistent with ^{31}P chemical shifts reported for other azaylides.[16] By contrast, no comparable intermediate accumulated in the reaction with benzyl azide. Conversion of azaylide **17a** to the ligation product was rather slow (>24 h at room temperature for complete conversion). This is in sharp contrast to the reaction with benzyl azide, wherein complete conversion of starting material (**7**) to the ligation product occurred within 35 min under the same conditions. Presumably, resonance stabilization of the phenyl-substituted azaylide **17a** (Scheme 4) reduces its reactivity relative to benzyl-substituted azaylide **10** (Scheme 3).

The reaction was repeated with *p*-methoxyphenyl azide (**16b**) and *p*-nitrophenyl azide (**16c**). The Staudinger ligation with **16b** was complete within 8 h, but the reaction with **16c** required more than 48 h for complete conversion. In all cases, the phosphine starting material was completely converted to the azaylide intermediate in <5 min. Collectively, these observations suggest that the rate-determining step in Staudinger ligation reactions with aryl azides is the intramolecular amide bond-forming step, rather than initial formation of the phosphazide as observed with benzyl azide. Presumably, this change in the rate-determining step is the consequence of enhanced azaylide stability due to resonance stabilization.

Characterization of a Reaction Intermediate under Anhydrous Conditions. We previously proposed the reaction pathway shown in Scheme 3, involving compound **11** as a key intermediate leading to the ligation product **12**.[2] In an earlier study, we did not observe the accumulation of any intermediate in reactions of phosphine **7** and benzyl azide in the presence of excess water.[4] However, we observed ^{31}P resonances corresponding to azaylide **10** (15 ppm) and a second intermediate that accumulated under anhydrous conditions or in the presence of substoichiometric amounts of water. On the basis of the ^{31}P NMR spectrum of this second intermediate and those reported for phosphetanes,[16] we proposed the bridged bicyclic oxazaphosphetane structure **18** shown in Scheme 5.[4] Addition of water to the intermediate led to formation of ligation product **12**. Since our structural assignment was based on limited analytical data, we undertook a more thorough characterization of the intermediate by NMR and X-ray analysis.

The intermediate was isolated from the reaction of **7** and benzyl azide in CH_2Cl_2 under rigorously anhydrous conditions

Scheme 5

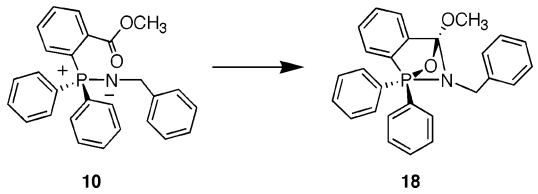

10 18

(glovebox). The ^{1}H NMR spectrum (Figure 4A) was not consistent with that of the previously proposed structure **18**. The resonance corresponding to the methoxy protons (3.03 ppm) was an apparent doublet with a relatively large *J*-coupling constant of 11 Hz (Figure 4A, top). Broadband ^{31}P decoupling collapsed the doublet into a singlet (Figure 4A, bottom), indicating coupling of the methoxy protons to the ^{31}P nucleus. In oxazaphosphetane **18**, the methoxy protons should not exhibit such a large coupling to the phosphorus nucleus.

Furthermore, the 2D ^{1}H−^{13}C HMBC spectrum (Figure 4B) of the isolated intermediate did not show a $^{3}J_{H-C}$ cross-peak between the methoxy protons (3.03 ppm) and the carbonyl carbon (δ 165 ppm), arguing against **18** as the correct structure. On the basis of these results, we propose a new structure for the intermediate, namely, pentacoordinate phosphorane **19** (Figure 4C), which is consistent with the observed NMR data. The connectivity of the intermediate was further confirmed by X-ray crystallography (Figure 4C). In the solid state, the three large phenyl substituents occupy the equatorial positions, whereas the two more electronegative substituents occupy the apical positions. The bond angles around the phosphorus center are close to those predicted for the trigonal bipyramidal geometry without significant distortion.

Addition of water to compound **19** resulted in the formation of Staudinger ligation product **12** (Scheme 3). As shown in Scheme 6, we propose a mechanism for this reaction that involves the initial formation of phosphonium intermediate **20**. Presumably, this intermediate also forms during the Staudinger ligation in aqueous media (Scheme 3) but is trapped by water rather than methanol under these circumstances. In either case, the oxygen atom of the phosphine oxide in the ligation product should originate from water via the intermediacy of phosphorane **21**.

To test this hypothesis, the isolated phosphorane intermediate **19** was hydrolyzed with ^{17}O/^{18}O-enriched water (76.7% ^{17}O, 10.5% ^{16}O, and 12.8% ^{18}O). The ^{31}P NMR spectra of the hydrolysis products from either unlabeled (top) or labeled (bottom) water are shown in Figure 5. A broad peak from 30 to 36 ppm was observed in the bottom spectrum, which we attribute to a ^{31}P nucleus coupled to ^{17}O. The significant broadening of the phosphorus resonance is a result of its fast spin−spin relaxation (short T_2) induced by the quadrupolar ^{17}O nucleus.[19] Two additional closely spaced ^{31}P resonances were also observed, corresponding to ^{31}P nuclei bound to either ^{16}O or ^{18}O. ^{16}O and ^{18}O are not NMR active; therefore, the ^{31}P resonances appear as singlets. The slight difference in chemical shifts of the two ^{31}P resonances is the result of an isotope effect.[20] Mass spectrometry analysis further confirmed the presence of heavy oxygen isotopes in the Staudinger ligation product (data not shown). These experiments provide direct evidence for the mechanism of phosphorane hydrolysis shown

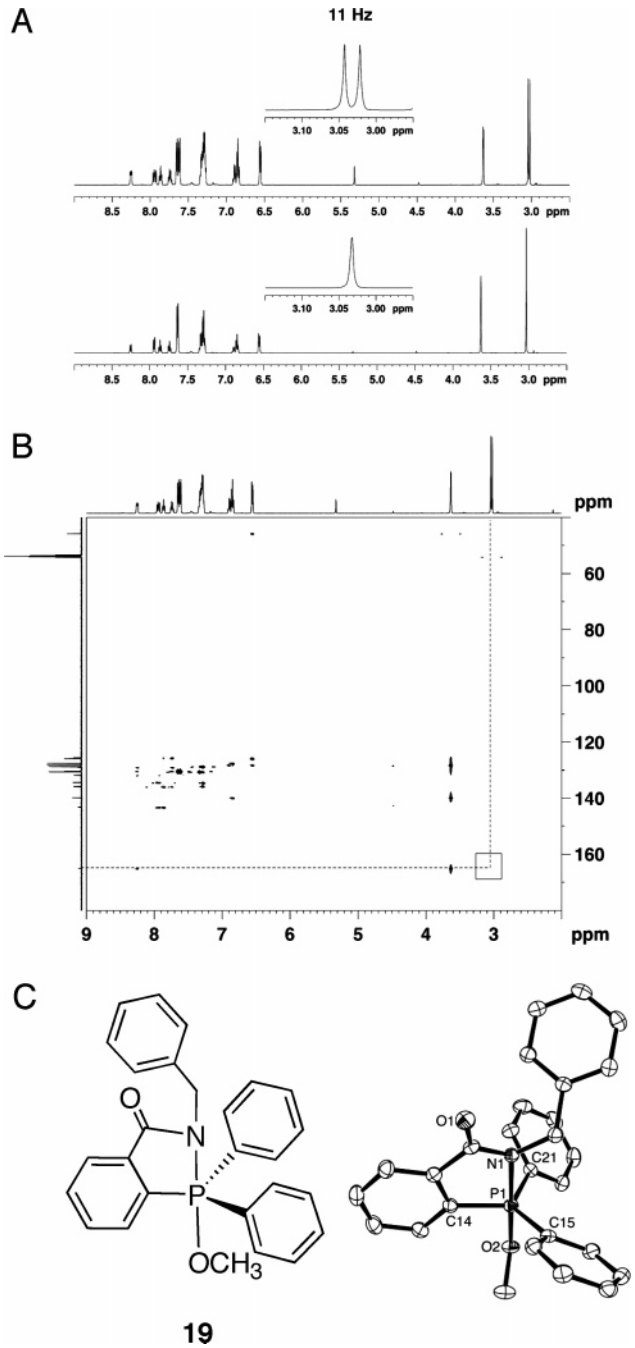

Figure 4. Characterization of intermediate **19**. (A) (top) ^{1}H spectrum of intermediate **19** isolated from the reaction of phosphine **7** (0.40 M) and benzyl azide (**8**) (0.44 M) in CH_2Cl_2 in the absence of water. The doublet at 3.03 ppm corresponds to the methoxy group; (bottom) ^{1}H{^{31}P} spectrum of **19**. (B) 2D ^{1}H−^{13}C HMBC spectrum of intermediate **19**. Note the absence of the cross-peak between the methoxy protons (3.03 ppm) and carbonyl carbon (165 ppm) that would have been expected for structure **18**. (C) Schematic and ORTEP diagrams illustrating the geometry and atom labeling scheme for intermediate **19** (hydrogen atoms have been omitted for clarity). Selected bond lengths (Å) and angles (deg): P−O(2) = 1.687(1), P−N = 1.903(1), P−C(14) = 1.817(2), P−C(15) = 1.826(2), P−C(21) = 1.823-(2), O(2)−P−N = 178.39(6), O(2)−P−C(14) = 96.02(7), O(2)−P−C(15) = 93.88(7), O(2)−P−C(21) = 88.48(7), N−P−C(14) = 84.40(7), N−P−C(15) = 87.27(7), N−P−C(21) = 89.94(7), C(14)−P−C(15) = 118.73-(8), C(14)−P−C(21) = 116.25(8), C(15)−P−C(21) = 124.33(8).

(19) Boykin, D. W. *^{17}O NMR Spectroscopy in Organic Chemistry*; CRC Press: New York, 1990.
(20) Quin, L. D.; Verkade, J. G. *Phosphorus-31 NMR Spectral Properties in Compound Characterization and Structural Analysis*; VCH: New York, 1994.

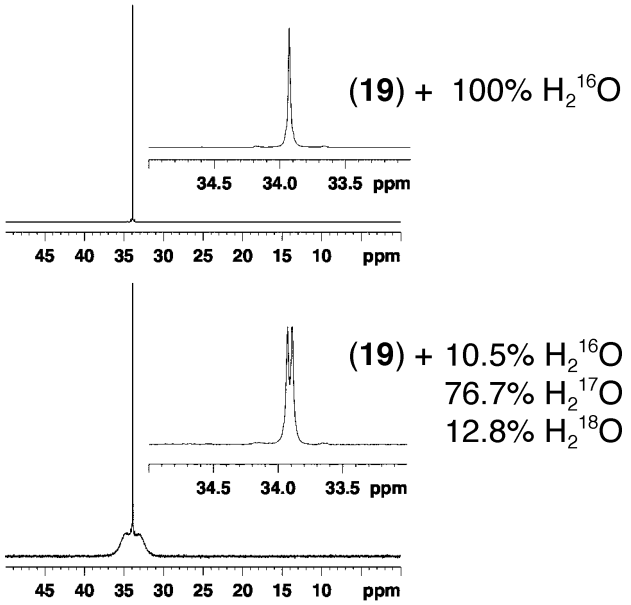

Figure 5. $^{31}P\{^1H\}$ spectra of the Staudinger ligation products obtained from the hydrolysis of intermediate **19** using either H_2O (top) or $^{17}O/^{18}O$-enriched H_2O (bottom).

Scheme 6

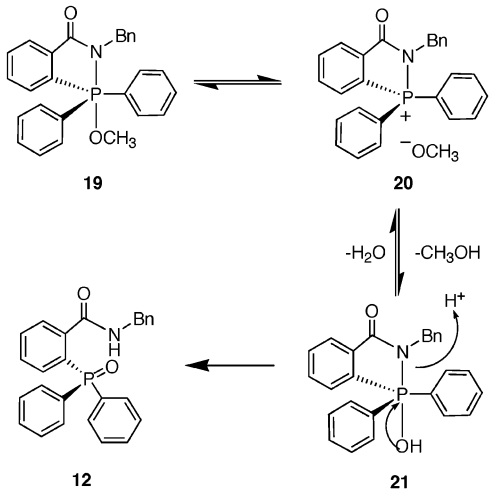

in Scheme 6, wherein the oxygen atom of the phosphine oxide originates from water.

Conclusions

In summary, we have identified parameters that affect the rate and yield of the Staudinger ligation and defined intermediates along the reaction pathway. Our results demonstrate that the overall rate of the reaction is dependent on the electronic properties of both the phosphine and the azide, making it possible to tune the reactivity of the substrates for rate enhancement. Moreover, the reaction tolerates a range of ester leaving groups, although significant addition of steric bulk can direct the reaction toward azaylide hydrolysis products at the expense of ligation products. Still, several alkyl and aryl alcohols function as efficient leaving groups, and these might be engineered for specific biological applications. For example, the leaving groups could be designed with chromogenic or fluorogenic properties or used as prodrugs. The Staudinger ligation shows some sensitivity to solvent polarity and is expected to proceed most rapidly in polar, protic solvents, such as water. This bodes well for most biological applications, although reactions in lipophilic environments, such as membranes, might be compromised. More generally, these results provide a framework for tailoring the Staudinger ligation for specific purposes.

Experimental Section

General. All chemical reagents were of analytical grade, obtained from commercial suppliers (Sigma-Aldrich for chemicals, Cambridge Isotope Laboratories for deuterated solvents, and Isotec for $^{17}O/^{18}O$-enriched water), and used without further purification. All Pd-catalyzed cross-coupling reactions were performed under Ar using standard Schlenk techniques. Reaction vessels were flame-dried prior to use. Flash chromatography was performed using Merck 60 Å 230−400 mesh silica gel. Analytical TLC was performed on Analtech Uniplate silica gel plates and visualized by staining with ceric ammonium molybdate or by absorbance of UV light at 254 nm. Acetonitrile (CH_3CN), deuterated acetonitrile (CD_3CN), and triethylamine (TEA) were distilled over calcium hydride, and methanol (MeOH) was dried over Mg°. All solvents for Pd-catalyzed cross-coupling reactions and NMR studies were degassed by three freeze−pump−thaw cycles and stored under Ar. All organic extracts were dried over Na_2SO_4, filtered, and concentrated under reduced pressure using a rotary evaporator.

^1H NMR, $^{13}C\{^1H\}$ NMR, and $^{31}P\{^1H\}$ NMR spectra were obtained with Bruker Avance AV-400 (9.4 T) or Bruker DRX-500 (11.7 T) spectrometers equipped with a 5 mm *z*-gradient broadband probe. ^{19}F NMR spectra were obtained with a Bruker Avance 400 spectrometer equipped with a 5 mm *z*-gradient QNP probe. ^1H and ^{13}C chemical shifts (δ) are reported in parts per million (ppm) referenced to TMS (0 ppm) and were measured relative to the residual solvent peak. ^{31}P chemical shifts are referenced to 85% H_3PO_4 in D_2O (0 ppm) and were measured relative to trimethyl phosphate in C_6D_6 (3.0 ppm). ^{19}F chemical shifts are referenced to $CFCl_3$ (0 ppm). Coupling constants (J) are reported in hertz (Hz). Due to ^{31}P coupling, resonances for certain carbon atoms in the phosphines listed below were observed as doublets. One-dimensional ^{13}C spectra with broadband ^1H and ^{31}P decoupling were obtained for representative compounds to identify the carbon resonances that are coupled to ^{31}P. These spectra were recorded on a Bruker Avance AV-500 spectrometer equipped with a 5 mm triple-resonance, broadband, inverse probe with *xyz* gradients. J_{CP} values were measured from the 1D $^{13}C\{^1H\}$ spectra and are reported in hertz.

IR spectral data were obtained using a Perkin-Elmer 1600 FTIR spectrometer. Low- and high-resolution fast atom bombardment (FAB) and electrospray ionization (ESI) mass spectra were obtained at the UC—Berkeley Mass Spectrometry Laboratory, and elemental analyses were obtained at the UC—Berkeley Microanalytical Laboratory. Melting points were determined using a Mel-Temp 3.0 melting point apparatus and are uncorrected.

Synthetic Procedures and Spectral Data for Phosphines.[21−23] Compounds 13a−d. The compounds with varied ester substituents were prepared by Pd(II)-mediated coupling of diphenylphosphine with the corresponding *o*-iodobenzoate esters, essentially as described by Saxon et al.[4]

2-Diphenylphosphanyl Benzoic Acid Methyl Ester (13a). To a solution of methyl 2-iodobenzoate (4.90 g, 18.7 mmol) dissolved in 20 mL of anhydrous, degassed CH_3CN were added anhydrous TEA (2.87 mL, 20.6 mmol), $Pd(OAc)_2$ (42.0 mg, 0.187 mmol), and 1,3-bisdiphenylphosphinopropane (dppp) (77.0 mg, 0.187 mmol). Diphenylphosphine (5.0 mL, 18 mmol) was added to the mixture slowly via syringe, upon which the solution turned deep red. The solution was heated at reflux for 4 h, after which the reaction was complete, as indicated by TLC analysis. The reaction mixture was cooled to 25 °C, and excess solvent was removed in vacuo to yield a red solid. The

crude product was purified by flash chromatography (1:9 EtOAc/hexanes) under N_2 to yield a white solid. This solid was further purified by recrystallization from MeOH to yield 4.6 g (76%) of a white crystalline solid: mp 99−100 °C (lit.[4] 96 °C); ^{1}H NMR (500 MHz, $CDCl_3$) δ 3.75 (s, 3), 6.92−6.98 (m, 1), 7.26−7.84 (m, 12), 8.03−8.07 (m, 1); ^{13}C NMR (125 MHz, $CDCl_3$) δ 52.32, 128.57, 128.73, 128.79, 129.00, 130.96, 132.23, 134.06, 134.22, 134.59, 167.46; ^{31}P NMR (162 MHz, $CDCl_3$) δ −4.5. FAB−HRMS calcd for $C_{20}H_{17}O_2P$: *m*/*z* 321.1044, found 321.1127. Anal. Calcd for $C_{20}H_{17}O_2P$: C, 74.99; H, 5.38. Found: C, 74.98; H, 5.38.

2-Diphenylphosphanyl Benzoic Acid Ethyl Ester (13b). The procedure was similar to that described for **13a**. The reaction was performed with 1.95 g (7.06 mmol) of 2-iodobenzoic acid ethyl ester and 1.3 mL (7.0 mmol) of diphenylphosphine, and 0.80 g (34%) of a white crystalline solid was obtained after recrystallization from MeOH: mp 114 °C; ^{1}H NMR (500 MHz, $CDCl_3$) δ 1.20 (t, 3, J = 7.0), 4.22 (q, 2, J = 7.0), 6.92−6.94 (m, 1), 7.26−7.42 (m, 12), 8.05−8.07 (m, 1); ^{13}C NMR (125 MHz, $CDCl_3$) δ 14.02, 61.20, 128.21, 128.41, 128.46, 130.59, 131.81, 133.80, 133.96, 134.29, 134.61, 137.75, 137.83, 166.87; ^{31}P NMR (162 MHz, $CDCl_3$) δ −4.7; IR (thin film, cm^{-1}) ν 3056, 2796, 1709, 1430, 1269, 1102. FAB−LRMS calcd for $C_{21}H_{19}O_2P$: *m*/*z* 334.1, found $[M + H]^+$ 335.1. Anal. Calcd for $C_{21}H_{19}O_2P$: C, 75.44; H, 5.35. Found: C, 75.63; H, 5.75.

2-Diphenylphosphanyl Benzoic Acid Isopropyl Ester (13c). The procedure was similar to that described for **13a**. The reaction was performed with 1.34 g (4.62 mmol) of 2-iodobenzoic acid isopropyl ester and 1.3 mL (5.1 mmol) of diphenylphosphine to give 0.60 g (37%) of a white crystalline solid after recrystallization from MeOH: mp 98−100 °C; ^{1}H NMR (400 MHz, $CDCl_3$) δ 1.19 (d, 6, J = 6.4), 5.12 (app septet, 1, J = 6.4), 6.92−6.95 (m, 1), 7.28−7.88 (m, 12), 8.04−8.07 (m, 1); ^{13}C NMR (125 MHz, $CDCl_3$) δ 21.55, 68.75, 127.98, 128.25 (d, J_{CP} = 7.2), 130.32, 131.49, 133.77 (d, J_{CP} = 20.6), 134.08, 135.30 (d, J_{CP} = 11.2), 138.04 (d, J_{CP} = 11.5), 139.70 (d, J_{CP} = 26.4), 166.28 (d, J_{CP} = 2.2); ^{31}P NMR (162 MHz, $CDCl_3$) δ −4.9; IR (thin film, cm^{-1}) ν 3062, 2981, 1703, 1263, 1102. FAB−LRMS calcd for $C_{22}H_{21}O_2P$: *m*/*z* 348, found $[M + H]^+$ 349. Anal. Calcd for $C_{22}H_{21}O_2P$: C, 75.85; H, 6.08. Found: C, 75.94; H, 6.12.

2-Diphenylphosphanyl Benzoic Acid *tert*-Butyl Ester (13d). The procedure was similar to that described for **13a**. The reaction was performed with 4.2 g (14 mmol) of 2-iodobenzoic acid *tert*-butyl ester and 3.8 mL (15 mmol) of diphenylphosphine to give 3.0 g (60%) of a white crystalline solid after recrystallization from MeOH: mp 127−128 °C; ^{1}H NMR (400 MHz, $CDCl_3$) δ 1.17 (s, 9), 6.89−6.92 (m, 1), 7.29−7.53 (m, 12), 7.95−7.98 (m, 1); ^{13}C NMR (125 MHz, $CDCl_3$) δ 27.82, 82.12, 128.21, 128.37, 128.42, 128.64, 130.29, 131.31, 133.88, 134.04, 166.51; ^{31}P NMR (162 MHz, $CDCl_3$) δ −4.4; IR (thin film, cm^{-1}) ν 3062, 2981, 1703, 1598, 1437, 1294. FAB−LRMS calcd for $C_{23}H_{23}O_2P$: *m*/*z* 362, found $[M + H]^+$ 363. Anal. Calcd for $C_{23}H_{23}O_2P$: C, 76.23; H, 6.40. Found: C, 76.22; H, 6.40.

Synthesis and Spectral Data for Phosphines 14a−f. Compounds **14a−f** were prepared by dicyclohexyl carbodiimide (DCC)-mediated coupling of diphenylphosphanyl benzoic acid with the corresponding phenol derivatives.

2-Diphenylphosphanyl Benzoic acid 4-Methoxyphenyl Ester (14a). 2-Diphenylphosphanyl benzoic acid (367 mg, 1.20 mmol) was dissolved in 50 mL of anhydrous CH_2Cl_2 under Ar. DCC (247 mg, 1.20 mmol) and DMAP (7.32 mg, 0.060 mmol) were added, and the reaction mixture was stirred at room temperature for 30 min. 4-Methoxyphenol (148 mg, 1.20 mmol) was added, and the resulting mixture was stirred at room temperature overnight. The reaction mixture was then concentrated to yield a slightly yellow solid. Ice-cold acetone was added to dissolve the crude product, and the insoluble urea byproduct was removed by filtration. The filtrate was concentrated, the residue purified by silica gel chromatography (1:9 EtOAc/hexanes), and the product recrystallized from MeOH to yield 200 mg (39%) of a white crystalline solid: mp 169−170 °C; ^{1}H NMR (500 MHz, $CDCl_3$) δ 3.78 (s, 3), 6.78−6.87 (m, 4), 6.98−7.00 (m, 1), 7.28−7.37 (m, 10), 7.43−7.52 (m, 2), 8.24−8.27 (m, 1); ^{13}C NMR (125 MHz, $CDCl_3$) δ 55.81, 114.56, 122.62, 128.52, 128.74, 128.80, 128.96, 311.50, 132.65, 133.96, 134.21, 134.61, 137.90, 141.51, 144.26, 157.45, 165.86; ^{31}P NMR (162 MHz, $CDCl_3$) δ −4.3; IR (thin film, cm^{-1}) ν 2919, 2857, 1728, 1499, 1238, 1189, 1040. FAB−LRMS calcd for $C_{26}H_{21}O_3P$: *m*/*z* 412.4, found $[M + H]^+$ 413.4. Anal. Calcd for $C_{26}H_{21}O_3P$: C, 75.72; H, 5.13. Found: C, 75.80; H, 4.74.

2-Diphenylphosphanyl Benzoic Acid 4-Tolyl Ester (14b). The procedure was similar to that described for **14a**. The reaction was performed with 430 mg (1.40 mmol) of 2-diphenylphosphanyl benzoic acid and 152 mg (1.40 mmol) of *p*-cresol to afford 500 mg (91%) of a white crystalline solid: mp 140−141 °C; ^{1}H NMR (500 MHz, $CDCl_3$) δ 2.32 (s, 3), 6.81−6.83 (m, 2), 6.98−7.00 (m, 1), 7.10−7.12 (m, 2), 7.28−7.37 (m, 11), 7.42−7.49 (m, 2), 8.25−8.27 (m, 1); ^{13}C NMR (125 MHz, $CDCl_3$) δ 20.80, 121.25, 128.24, 128.47 (d, J_{CP} = 7.3), 128.67, 129.74, 131.20 (d, J_{CP} = 2.9), 132.31, 133.78 (d, J_{CP} = 18.3), 134.02 (d, J_{CP} = 20.5), 134.33, 135.30, 137.70 (d, J_{CP} = 11.0), 141.15 (d, J_{CP} = 27.1), 148.33, 165.40 (d, J_{CP} = 2.9); ^{31}P NMR (162 MHz, $CDCl_3$) δ −4.3; IR (thin film, cm^{-1}) ν 3062, 1722, 1499, 1431, 1239, 1189, 1083, 1033. FAB−LRMS calcd for $C_{26}H_{21}O_2P$: *m*/*z* 396, found $[M + H]^+$ 397. Anal. Calcd for $C_{26}H_{21}O_2P$: C, 78.78; H, 5.34. Found: C, 78.39; H, 5.36.

2-Diphenylphosphanyl Benzoic Acid Phenyl Ester (14c). The procedure was similar to that described for **14a**. The reaction was performed with 220 mg (0.71 mmol) of 2-diphenylphosphanyl benzoic acid and 67 mg (0.71 mmol) of phenol to afford 220 mg (77%) of pale yellow crystals: mp 126−127 °C; ^{1}H NMR (500 MHz, $CDCl_3$) δ 6.94−7.00 (m, 2), 7.00−7.01 (m, 1), 7.17−7.20 (m, 1), 7.26−7.35 (m, 13), 7.36−7.49 (m, 2), 8.25−8.28 (m, 1); ^{13}C NMR (125 MHz, $CDCl_3$) δ 121.59, 125.72, 128.25, 128.45, 128.51, 128.69, 129.24, 131.24, 132.41, 133.48, 133.92, 134.08, 134.37, 137.60, 137.68, 141.16, 141.38, 150.52, 165.18; ^{31}P NMR (162 MHz, $CDCl_3$) δ −4.3; IR (thin film, cm^{-1}) ν 1728, 1586, 1238, 1189, 1090, 1040. FAB−LRMS calcd for $C_{25}H_{19}O_2P$: *m*/*z* 382, found $[M + H]^+$ 383. Anal. Calcd for $C_{25}H_{19}O_2P$: C, 78.52; H, 5.01. Found: C, 78.37; H, 4.84.

2-Diphenylphosphanyl Benzoic Acid 4-Fluorophenyl Ester (14d). The procedure was similar to that described for **14a**. The reaction was performed with 362 mg (1.18 mmol) of 2-diphenylphosphanyl benzoic acid and 132 mg (1.18 mmol) of *p*-fluorophenol to afford 340 mg (71%) of white crystals: mp 109−110 °C; ^{1}H NMR (500 MHz, $CDCl_3$) δ 6.88−6.92 (m, 2), 6.97−7.02 (m, 3), 7.28−7.36 (m, 10), 7.44−7.50 (m, 2), 8.23−8.24 (m, 1); ^{13}C NMR (125 MHz, $CDCl_3$) δ 115.77, 115.96, 122.94, 123.01, 128.30, 128.53 (d, J_{CP} = 7.7), 128.77, 131.24 (d, J_{CP} = 2.2), 132.52 (d, J_{CP} = 17.6), 134.00 (d, J_{CP} = 20.5), 134.40, 137.52 (d, J_{CP} = 11.0), 141.25 (d, J_{CP} = 27.8), 146.25, 159.07, 161.50, 165.34 (d, J_{CP} = 2.2); ^{31}P NMR (162 MHz, $CDCl_3$) δ −4.2; ^{19}F NMR (376 MHz, $CDCl_3$) δ −116.20 (m); IR (thin film, cm^{-1}) ν 3056, 2956, 1735, 1499, 1430, 1244, 1182, 1090, 1040. FAB−LRMS calcd for $C_{25}H_{18}FO_2P$: *m*/*z* 400, found $[M + H]^+$ 401. Anal. Calcd for $C_{25}H_{18}FO_2P$: C, 75.00; H, 4.53. Found: C, 75.13; H, 4.35.

2-Diphenylphosphanyl Benzoic Acid 4-Chlorophenyl Ester (14e). The procedure was similar to that described for **14a**. The reaction was performed with 350 mg (1.15 mmol) of 2-diphenylphosphanyl benzoic acid and 147 mg (1.15 mmol) of *p*-chlorophenol to afford 210 mg (43%) of a white crystalline solid: mp 153−154 °C; ^{1}H NMR (500 MHz, $CDCl_3$) δ 6.87−6.88 (m, 2), 6.98−7.02 (m, 1), 7.29−7.34 (m, 12), 7.44−7.50 (m, 2), 8.23−8.26 (m, 1); ^{13}C NMR (125 MHz, $CDCl_3$) δ 122.97, 128.30, 128.52, 128.79, 129.31, 131.12, 131.30, 132.63, 133.02, 133.92, 134.08, 134.41, 137.40, 137.49, 141.28, 141.50, 148.93, 164.98; ^{31}P NMR (162 MHz, $CDCl_3$) δ −4.1; IR (thin film, cm^{-1}) ν 3062, 2957, 2864, 1735, 1480, 1431, 1239, 1195, 1083, 1033. FAB−LRMS calcd for $C_{25}H_{18}ClO_2P$: *m*/*z* 416, found $[M + H]^+$ 417. Anal. Calcd for $C_{25}H_{18}ClO_2P$: C, 72.03; H, 4.35. Found: C, 72.00; H, 4.35.

2-Diphenylphosphanyl Benzoic Acid 4-Nitrophenyl Ester (14f). The procedure was similar to that described for **14a**. The reaction was

performed with 500 mg (1.63 mmol) of 2-diphenylphosphanyl benzoic acid and 227 mg (1.63 mmol) of *p*-nitrophenol to afford 400 mg (60%) of a pale yellow solid: mp 111−113 °C; ^{1}H NMR (400 MHz, $CDCl_3$) δ 7.00−7.03 (m, 1), 7.08−7.13 (m, 2), 7.29−7.38 (m, 10), 7.47−7.51 (m, 2), 8.15−8.26 (m, 3); ^{13}C NMR (125 MHz, $CDCl_3$) δ 122.42, 125.01, 128.39, 128.63, 128.94 (d, J_{CP} = 7.3), 131.44 (d, J_{CP} = 2.2), 132.52 (d, J_{CP} = 17.6), 132.99, 134.01, 134.53 (d, J_{CP} = 20.5), 137.20 (d, J_{CP} = 10.2), 141.76 (d, J_{CP} = 27.8), 145.30, 155.25, 164.28 (d, J_{CP} = 2.9); ^{31}P NMR (162 MHz, $CDCl_3$) δ −3.7. FAB−LRMS calcd for $C_{25}H_{18}NO_4P$: *m*/*z* 427, found $[M + H]^+$ 428. Anal. Calcd for $C_{25}H_{18}NO_4P$: C, 70.26; H, 4.25; N, 3.28. Found: C, 69.90; H, 4.06; N, 3.24.

Synthesis and Spectral Data for Phosphines 15a−f. The unsymmetrical phosphines were synthesized using a procedure similar to that described in refs 22 and 23. Briefly, methyl 2-iodobenzoate and phenylphosphine were coupled using $Pd(OAc)_2$. The diarylphosphine was then coupled in a manner similar to that of the appropriate aryl iodide to afford the triarylphosphine product.

2-[(4-*N*,*N*-(Dimethylamino)phenyl)phenylphosphanyl] Benzoic Acid Methyl Ester (15a). To a solution of methyl 2-iodobenzoate (4.0 g, 15 mmol) dissolved in 100 mL of anhydrous and degassed CH_3CN were added anhydrous TEA (23 mL, 15 mmol), $Pd(OAc)_2$ (110 mg, 0.5 mmol), and 1,3-bisdiphenylphosphinopropane (dppp) (206 mg, 0.5 mmol). Phenylphosphine (1.7 mL, 15 mmol) was added to the above mixture over a 5 min period via syringe, during which time the solution turned deep red. The reaction mixture was heated at reflux, and reaction progress was monitored by ^{31}P NMR. A new ^{31}P resonance at about −48 ppm was observed after 30 min, consistent with formation of a secondary phosphine.[20] The reaction mixture was heated for 10 h, at which point most of the phenylphosphine was consumed (∼70%), as determined by ^{31}P NMR analysis. Complete conversion to the diaryl phosphine could not be achieved even after prolonged heating (>24 h). The diaryl phosphine was carried on to the next step without purification. The reaction mixture was cooled to 25 °C, and a second equivalent of TEA (0.77 mL, 0.55 mmol) and *N*,*N*-(dimethylamino)-4-iodobenzene (3.8 g, 15 mmol) was added. The resulting mixture was heated at reflux for 14 h, after which TLC and ^{31}P NMR analysis indicated complete consumption of the diaryl phosphine. The crude mixture was concentrated, and the product was purified by silica gel chromatography (1:9 EtOAc/hexanes) and recrystallization from MeOH to give 1.0 g (18%) of a yellow crystalline solid: mp 113−114 °C; ^{1}H NMR (500 MHz, $CDCl_3$) δ 2.97 (s, 6), 3.73 (s, 3), 6.70 (d, 2), 7.01−7.03 (m, 1), 7.18−7.39 (m, 9), 8.01−8.03 (m, 1); ^{13}C NMR (125 MHz, $CDCl_3$) δ 40.16, 51.81, 111.13, 112.37, 127.77, 128.04, 128.21 (d, J_{CP} = 6.6), 130.49 (d, J_{CP} = 2.2), 131.46, 131.64, 133.22 (d, J_{CP} = 19.8), 133.29, 134.03, 134.16 (d, J_{CP} = 18.3), 135.66 (d, J_{CP} = 22.7), 139.17 (d, J_{CP} = 8.8), 141.62 (d, J_{CP} = 27.1), 167.39 (d, J_{CP} = 2.9); ^{31}P NMR (202 MHz, $CDCl_3$) δ −7.0; IR (thin film, cm^{-1}) ν 3056, 2950, 1716, 1269, 1102, 1058. ESIMS calcd for $C_{22}H_{22}NO_2P$: *m*/*z* 363.1, found $[M + H]^+$ 364.1. Anal. Calcd for $C_{22}H_{22}NO_2P$: C, 72.71; H, 6.10; N, 3.85. Found: C, 72.64; H, 5.93; N, 3.87.

2-[(4-Hydroxyphenyl)phenylphosphanyl] Benzoic Acid Methyl Ester (15b). The procedure was similar to that described for **15a**. The reaction was performed with 2.6 g (10 mmol) of methyl 2-iodobenzoate, 1.1 mL (10 mmol) of phenylphosphine, and 2.8 g (10 mmol) of 4-iodophenol to afford 457 mg (6%) of pale yellow crystals: mp 113−114 °C; ^{1}H NMR (500 MHz, $CDCl_3$) δ 3.73 (s, 3), 6.78 (d, 2), 6.93−6.96 (m, 1), 7.15−7.18 (m, 2), 7.25−7.39 (m, 7), 8.02−8.05 (m, 1); ^{13}C NMR (100 MHz, $CDCl_3$) δ 52.09, 115.75, 115.83, 123.10, 128.42, 128.49, 130.71, 131.94, 133.45, 133.65, 134.12, 134.28, 135.80, 136.02, 156.48; ^{31}P NMR (162 MHz, $CDCl_3$) δ −5.9; IR (thin film, cm^{-1}) ν 3056, 2950, 1716, 1269, 1102, 1058. ESIMS calcd for $C_{20}H_{17}O_3P$: *m*/*z* 336.1, found $[M + H]^+$ 337.1. Anal. Calcd for $C_{20}H_{17}O_3P$: C, 71.42; H, 5.09. Found: C, 71.11; H, 5.15.

2-[(4-Methoxyphenyl)phenylphosphanyl] Benzoic Acid Methyl Ester (15c). The procedure was similar to that described for **15a**. The reaction was performed with 1.31 g (5 mmol) of methyl 2-iodobenzoate, 0.55 mL (5 mmol) of phenylphosphine, and 1.17 g (5 mmol) of 4-iodoanisole to afford 105 mg (6%) of an off-white solid (mp 89−90 °C) after two rounds of flash chromatography (1:9 EtOAc/hexanes) under N_2: ^{1}H NMR (400 MHz, $CDCl_3$) δ 3.75 (s, 3), 3.82 (s, 3), 6.88−6.90 (m, 2), 6.95−6.98 (m, 1), 7.23−7.40 (m, 9), 8.03−8.06 (m, 1); ^{13}C NMR (125 MHz, $CDCl_3$) δ 52.27, 55.38, 114.43, 114.50, 128.39, 128.64, 128.69, 128.74, 132.14, 133.62, 133.78, 134.39, 161.51; ^{31}P NMR (162 MHz, $CDCl_3$) δ −5.9; IR (thin film, cm^{-1}) ν 2950, 2832, 1716, 1585, 1499, 1430, 1288, 1244. 1176. ESIMS calcd for $C_{21}H_{19}O_3P$: *m*/*z* 350.1, found $[M + H]^+$ 351.1. Anal. Calcd for $C_{21}H_{19}O_3P$: C, 71.99; H, 5.47. Found: C, 71.76; H, 5.49.

2-[(4-Methylphenyl)phenylphosphanyl] Benzoic Acid Methyl Ester (15d). The procedure was similar to that described for **15a**. The reaction was performed with 1.3 g (5 mmol) of methyl 2-iodobenzoate, 0.55 mL (5 mmol) of phenylphosphine, and 1.2 g (5 mmol) of 4-iodotoluene to afford 124 mg (7%) of a bright yellow oil after purification by silica gel chromatography (1:9 EtOAc/hexanes): ^{1}H NMR (500 MHz, $CDCl_3$) δ 2.36 (s, 3), 3.75 (s, 3), 6.94−6.97 (m, 1), 7.15−7.21 (m, 4), 7.28−7.40 (m, 7), 8.04−8.06 (m, 1); ^{13}C NMR (125 MHz, $CDCl_3$) δ 21.30, 51.98, 128.04, 128.36, 128.41, 128.46, 129.29, 129.35, 130.63, 131.84, 133.59, 133.75, 133.90, 134.07, 134.18, 138.66, 154.01; ^{31}P NMR (162 MHz, $CDCl_3$) δ −5.9. ESIMS calcd for $C_{21}H_{20}O_2P$ $[M + H]^+$: *m*/*z* 334.1, found $[M + H]^+$ 335.1. FAB−HRMS calcd for $C_{21}H_{20}O_2P$ $[M + H]^+$: *m*/*z* 335.1201, found 335.1205.

2-[(4-Bromophenyl)phenylphosphanyl] Benzoic Acid Methyl Ester (15e). The procedure was similar to that described for **15a**. The reaction was performed with 2.6 g (10 mmol) of methyl 2-iodobenzoate, 1.1 mL (10 mmol) of phenylphosphine, and 2.8 g (10 mmol) of 1-bromo-4-iodobenzene to afford 457 mg (6%) of an off-white solid: mp 113−114 °C; ^{1}H NMR (500 MHz, $CDCl_3$) δ 3.82 (s, 3), 6.92−6.94 (m, 1), 7.27−7.39 (m, 2), 7.40−7.50 (m, 7), 8.13−8.16 (m, 3); ^{13}C NMR (125 MHz, $CDCl_3$) δ 52.05, 123.23, 128.40, 128.58 (d, J_{CP} = 7.3), 128.86, 130.76 (d, J_{CP} = 2.2), 131.59 (d, J_{CP} = 7.3), 132.05, 133.87, 134.16 (d, J_{CP} = 21.2), 135.30 (d, J_{CP} = 21.2), 137.28 (d, J_{CP} = 7.3), 137.34 (d, J_{CP} = 6.6), 139.88 (d, J_{CP} = 26.3), 167.05 (d, J_{CP} = 2.2); ^{31}P NMR (162 MHz, $CDCl_3$) δ −4.3; IR (thin film, cm^{-1}) ν 3056, 2950, 1716, 1269, 1102, 1058. ESIMS calcd for $C_{20}H_{16}BrO_2P$: *m*/*z* 399, found $[M + H]^+$ 400. Anal. Calcd for $C_{20}H_{16}BrO_2P$: C, 60.17; H, 4.04. Found: C, 60.12; H, 3.99.

2-[(4-Nitrophenyl)phenylphosphanyl] Benzoic Acid Methyl Ester (15f). The procedure was similar to that described for **15a**. The reaction was performed with 1.3 g (5 mmol) of methyl 2-iodobenzoate, 0.55 mL (5 mmol) of phenylphosphine, and 1.2 g (5 mmol) of 1-iodo-4-nitrobenzene to afford 124 mg (7%) of a bright yellow oil after purification by silica gel chromatography (1:9 EtOAc/hexanes): ^{1}H NMR (400 MHz, $CDCl_3$) δ 3.82 (s, 3), 6.92−6.94 (m, 1), 7.27−7.39 (m, 2), 7.40−7.50 (m, 7), 8.13−8.16 (m, 3); ^{13}C NMR (125 MHz, $CDCl_3$) δ 52.31, 123.08, 128.85, 128.91, 129.49, 130.94, 132.45, 133.72, 133.88, 134.28, 134.38, 134.55, 136.13, 136.22, 147.74, 148.22, 148.35, 166.93; ^{31}P NMR (162 MHz, $CDCl_3$) δ −4.3; IR (thin film, cm^{-1}) ν 2919, 2845, 1709, 1518, 1338, 1270, 1108. FAB−HRMS calcd for $C_{20}H_{17}NO_4P$ $[M + H]^+$: *m*/*z* 366.0895, found 366.0893.

Characterization of Staudinger Ligation Products from the Reactions of Phosphines 13a−d, 14a−f, and 15a−f and Benzyl Azide. The Staudinger ligation products formed in the reactions of benzyl azide with phosphines **13a−d**, **14a−f**, or **15a−f** were isolated from the reaction mixtures used in the kinetics experiments. During the course of these reactions, no background oxidation of the phosphines was observed.

(21) Quin, L. D. *A Guide to Organophosphorus Chemistry*; Wiley: New York, 2000.
(22) Brauer, D. J.; Hingst, M.; Kottsieper, K. W.; Liek, C.; Nickel, T.; Tepper, M.; Stelzer, O.; Sheldrick, W. S. *J. Organomet. Chem.* **2002**, *645*, 14−26.
(23) Herd, O. J.; Hessler, A.; Hingst, M.; Tepper, M.; Stelzer, O. *J. Organomet. Chem.* **1996**, *522*, 69−76.

***N*-Benzyl-2-(diphenylphosphinoyl)benzamide.**[4] This compound is the product of the Staudinger ligation of benzyl azide with phosphines **13a**−**d** and **14a**−**f**. The product was purified by silica gel chromatography (5:95 MeOH/CH_2Cl_2) and recrystallized from MeOH to yield a white solid: mp 195−196 °C; ^{1}H NMR (500 MHz, $CDCl_3$) δ 4.08−4.09 (d, 2, J = 5.5), 7.05−7.09 (dq, 1, J = 0.9, 7.7), 7.21−7.28 (m, 5), 7.35−7.39 (m, 1), 7.46−7.50 (m, 4), 7.55−7.67 (m, 7), 8.02−8.04 (dq, 1, J = 1.0, 4.0), 9.05−9.08 (br s, 1); ^{13}C NMR (125 MHz, $CDCl_3$) δ 44.00, 127.09, 127.92, 128.48, 128.66, 128.75, 128.93, 129.72, 129.75, 129.84, 130.59, 131.44, 131.61, 131.69, 131.75, 132.29, 132.32, 132.61, 133.34, 137.57, 140.98, 141.04, 167.21, 167.24; ^{31}P NMR (162 MHz, $CDCl_3$) δ 34.9; IR (thin film, cm^{-1}) ν 3050, 1660, 1579, 1480, 1437, 1300, 1172. EI−LRMS calcd for $C_{26}H_{22}NO_2P$: m/z 411, found (M^+) 411.

***N*-Benzyl-2-[(4-*N*,*N*-(dimethylamino)phenyl)phenylphosphinoyl]-benzamide.** This compound is the product of the Staudinger ligation of phosphine **15a** and benzyl azide. The product was purified by silica gel chromatography (5:95 MeOH/CH_2Cl_2) and recrystallized from MeOH to yield a white solid: mp 183−184 °C; ^{1}H NMR (500 MHz, $CDCl_3$) δ 3.02 (s, 6), 4.06−4.10 (dd, 1, J = 12.7, 5.3), 4.17−4.21 (dd, 1, J = 12.7, 5.3), 6.70−6.72 (d, 2, J = 11.0), 7.06−7.10 (m, 1), 7.17−7.64 (m, 14), 8.02−8.04 (dd, 1, J = 7.6, 2.2), 9.37−9.48 (m, 1); ^{13}C NMR (125 MHz, $CDCl_3$) δ 39.97, 44.06, 111.40, 111.51, 127.00, 127.92, 128.42, 128.49, 128.59, 129.60, 130.07, 130.84, 131.44, 131.52, 131.71, 131.77, 131.89, 132.22, 132.56, 133.07, 133.16, 133.26, 133.36, 137.76, 140.81, 140.87, 152.46, 167.55, 167.58; ^{31}P NMR (162 MHz, $CDCl_3$) δ 35.9. FAB−LRMS calcd for $C_{28}H_{27}N_2O_2P$: m/z 454, found $[M + H]^+$ 455. Anal. Calcd for $C_{28}H_{27}N_2O_2P$: C, 73.99; H, 5.99; N, 6.16. Found: C, 73.74; H, 6.09; N, 6.15.

***N*-Benzyl-2-[(4-hydroxy)phenylphosphinoyl]benzamide.** This compound is the product of the Staudinger ligation of phosphine **15b** and benzyl azide. The product was purified by silica gel chromatography (5:95 MeOH/CH_2Cl_2) and recrystallized from MeOH to yield a white solid: mp 194−195 °C; ^{1}H NMR (500 MHz, $CDCl_3$) δ 3.96−4.00 (dd, 1, J = 15.0, 4.0), 4.35−4.40 (dd, 1, J = 15.0, 6.0), 6.79−6.82 (m, 2), 7.04−7.09 (m, 1), 7.23−7.26 (m, 4), 7.37−7.70 (m, 10), 8.00−8.02 (m, 1), 9.36−9.37 (br s, 1); ^{13}C NMR (125 MHz, $CDCl_3$) δ 44.41, 116.30, 116.44, 120.04, 127.27, 127.89, 128.53, 128.65, 128.77, 129.75, 130.18, 130.30, 130.72, 131.38, 132.07, 132.17, 132.37, 132.65, 133.06, 133.18, 133.39, 133.51, 137.00, 140.09, 161.49, 168.81; ^{31}P NMR (162 MHz, $CDCl_3$) δ 36.1. FAB−LRMS calcd for $C_{26}H_{22}NO_3P$: m/z 427, found $[M + H]^+$ 428. Anal. Calcd for $C_{26}H_{22}NO_3P$: C, 73.06; H, 5.19; N, 3.28. Found: C, 72.73; H, 5.19; N, 3.59.

***N*-Benzyl-2-[(4-methoxyphenyl)phenylphosphinoyl]benzamide.** This compound is the product of the Staudinger ligation of phosphine **15c** and benzyl azide. The product was purified by silica gel chromatography (5:95 MeOH/CH_2Cl_2) and recrystallized from MeOH to yield a white solid: mp 209−210 °C; ^{1}H NMR (500 MHz, $CDCl_3$) δ 3.86 (s, 3) 4.10−4.15 (m, 2), 6.96−6.98 (m, 2), 7.05−7.09 (m, 1), 7.22−7.28 (m, 5), 7.41−7.67 (m, 9), 8.02−8.04 (m, 1), 9.18−9.21 (m, 1); ^{13}C NMR (125 MHz, $CDCl_3$) δ 44.06, 55.32, 114.28, 114.39, 122.14, 127.06, 127.95, 128.45, 128.62, 128.71, 130.09, 131.53, 131.61, 131.82, 131.87, 132.20, 133.52, 133.61, 137.61, 162.74, 167.90; ^{31}P NMR (202 MHz, $CDCl_3$) δ 34.1. FAB−LRMS calcd for $C_{27}H_{24}NO_3P$: m/z 441, found (M^+) 441. Anal. Calcd for $C_{27}H_{24}NO_3P$: C, 73.46; H, 5.48; N, 3.17. Found: C, 73.28; H, 5.52; N, 3.14.

***N*-Benzyl-2-[(4-methylphenyl)phenylphosphinoyl]benzamide.** This compound is the product of the Staudinger ligation of phosphine **15d** and benzyl azide. The product was purified by silica gel chromatography (5:95 MeOH/CH_2Cl_2) and recrystallized from MeOH to yield a white solid: mp 226−227 °C; ^{1}H NMR (500 MHz, $CDCl_3$) δ 2.42 (s, 3), 4.09−4.11 (m, 2), 7.06−7.11 (m, 1), 7.21−7.67 (m, 16), 8.02−8.06 (m, 1), 8.91−9.00 (m, 1); ^{13}C NMR (125 MHz, $CDCl_3$) δ 21.66, 44.02, 127.06, 127.94, 128.45, 128.62, 128.72, 129.12, 129.45, 129.55, 129.74, 131.56, 131.64, 131.70, 131.81, 132.23, 132.55, 133.32, 137.59, 142.94, 167.30; ^{31}P NMR (162 MHz, $CDCl_3$) δ 35.5. FAB−LRMS calcd for $C_{27}H_{24}NO_2P$: m/z 425, found $[M + H]^+$ 426. Anal. Calcd for $C_{27}H_{24}NO_2P$: C, 76.22; H, 5.69; N, 3.29. Found: C, 75.91; H, 5.84; N, 3.55.

***N*-Benzyl-2-[(4-bromophenyl)phenylphosphinoyl]benzamide.** This compound is the product of the Staudinger ligation of phosphine **15e** and benzyl azide. The product was purified by silica gel chromatography (5:95 MeOH/CH_2Cl_2) and recrystallized from MeOH to yield a white solid: mp 206−207 °C; ^{1}H NMR (500 MHz, $CDCl_3$) δ 4.06−4.18 (m, 2), 7.06−7.11 (m, 1), 7.21−7.67 (m, 16), 8.02−8.06 (m, 1), 8.91−8.98 (m, 1); ^{13}C NMR (125 MHz, $CDCl_3$) δ 44.06, 127.19, 127.58, 128.00, 128.31, 128.51, 128.77, 128.87, 129.11, 130.10, 131.59, 131.67, 131.74, 131.82, 131.98, 132.08, 132.53, 132.86, 132.99, 133.08, 133.23, 133.33, 137.45, 140.97, 167.08; ^{31}P NMR (162 MHz, $CDCl_3$) δ 34.7. FAB−LRMS calcd for $C_{26}H_{21}BrNO_2P$: m/z 490, found (M^+) 490. Anal. Calcd for $C_{26}H_{21}BrNO_2P$: C, 63.69; H, 4.32; N, 2.86. Found: C, 63.30; H, 4.45; N, 2.86.

***N*-Benzyl-2-[(4-nitrophenyl)phenylphosphinoyl]benzamide.** This compound is the product of the Staudinger ligation of phosphine **15f** and benzyl azide. The product was purified by silica gel chromatography (5:95 MeOH/CH_2Cl_2) and recrystallized from MeOH to yield a pale yellow solid: mp 142−144 °C; ^{1}H NMR (500 MHz, $CDCl_3$) δ 4.04−4.19 (m, 2), 7.14−7.26 (m, 5), 7.36−7.90 (m, 8), 8.00−8.02 (m, 1), 8.24−8.26 (m, 2), 8.54−8.57 (m, 1); ^{13}C NMR (125 MHz, $CDCl_3$) δ 44.07, 123.38, 123.48, 127.36, 128.11, 129.03, 130.09, 130.19, 131.71, 131.79, 132.60, 132.68, 132.87, 133.31, 137.25, 158.23; ^{31}P NMR (162 MHz, $CDCl_3$) δ 32.9. FAB−HRMS calcd for $C_{26}H_{22}N_2O_4P$ $[M + H]^+$: m/z 457.1317, found 457.1320.

Isolation and Characterization of Intermediate 19. All compounds were manipulated in a glovebox under an inert atmosphere (N_2). Glassware was dried overnight at 150 °C or flame-dried under vacuum immediately prior to use. NMR tubes were sealed by attaching the tube directly to a Kontes high-vacuum stopcock via a Cajon Ultra-Torr reducing union and flame-sealing on a vacuum line.

Anhydrous CH_2Cl_2, pentane, and diethyl ether were obtained by passage through a column of activated alumina (type A2, size 12 × 32, Purify Co.) under N_2 pressure, sparged with N_2, and stored over 3 Å molecular sieves in the glovebox under N_2. CD_2Cl_2 was dried over calcium hydride, degassed by three freeze−pump−thaw cycles, vacuum transferred to a glass bomb, and stored over 3 Å molecular sieves under an atmosphere of N_2. Benzyl azide was additionally dried over 3 Å sieves in a vial in the glovebox for 4 days prior to use.

A solution of phosphine **13a** (0.637 g, 1.99 mmol) and benzyl azide (0.295 g, 2.22 mmol) in CH_2Cl_2 (5.0 mL) was stirred at room temperature in the glovebox for 3 days. Upon mixing, vigorous bubbling was observed in the pale yellow solution. The volatile materials were removed under vacuum to yield a brown oil. Upon adding pentane (10 mL) to this oil, a white solid precipitated from the brown solution. The solid was dried under vacuum then washed twice with toluene (2 × 10 mL). The resulting off-white powder (mp 141−143 °C) was then dried under vacuum to yield compound **19** (0.662 g, 78%), which was analytically pure. A small amount of compound **19** (∼20 mg) was crystallized at −30 °C from diethyl ether (∼1.5 mL) to yield colorless bladelike crystals in the space group $P2_1/n$: ^{1}H NMR (500 MHz, CD_2Cl_2) δ 3.02−3.05 (d, 3, J = 11.0), 3.70−3.71 (d, 2, J = 4.0), 6.63−6.65 (d, 2, J = 8.0), 6.90−7.00 (m, 3), 7.22−7.50 (m, 6), 7.63−7.79 (m, 5), 7.92−7.98 (m, 1), 7.98−8.00 (m, 1), 8.33−8.35 (m, 1); ^{13}C NMR (125 MHz, CD_2Cl_2) δ 46.00, 54.17 (d, J_{CP} = 8.2), 125.62 (d, J_{CP} = 13.0), 125.83, 127.57, 128.21, 128.74 (d, J_{CP} = 16.8), 129.73 (d, J_{CP} = 159.3), 130.29 (d, J_{CP} = 3.4), 130.56 (d, J_{CP} = 11.0), 131.81 (d, J_{CP} = 15.4), 134.31 (d, J_{CP} = 3.4), 135.11 (d, J_{CP} = 170.8), 135.89 (d, J_{CP} = 11.5), 139.84, 143.28 (d, J_{CP} = 11.5), 165.10 (d, J_{CP} = 8.2); ^{31}P NMR (162 MHz, CD_2Cl_2) δ −56.0. ESI−LRMS calcd for $C_{27}H_{24}NO_2P$: m/z 425, found $[M + H]^+$ 426. Anal. Calcd for $C_{27}H_{24}NO_2P$: C, 76.22; H, 5.69; N, 3.29. Found: C, 76.11; H, 5.69; N, 3.44.

General Procedures for Kinetics Experiments using ^{31}P NMR Spectroscopy.[20] Stock solutions of phosphine, azide, and the internal standard (triphenylphosphine oxide) were prepared as follows. The phosphine was placed in a 1.00 mL volumetric tube, and anhydrous, degassed CD_3CN was added to yield a total volume of 1.00 mL and final phosphine concentrations between 0.064 and 0.26 M. Gentle heating in a water bath (~45 °C) was required to dissolve the phosphine completely. The phosphine stock solution was transferred to a flame-dried screw-capped vial, purged with Ar for 5 min, and stored at −20 °C until use. Stock solutions of the azide (4.95 M) and triphenylphosphine oxide (0.31 M) were prepared and stored in a similar manner.

In a typical experiment, 100 μL each of the phosphine and phosphine oxide stock solutions was transferred to a 5 mm NMR tube using a pipetman. Distilled water (30 μL, 1.7 mmol) and 270 μL of CD_3CN were added to give a final volume of 500 μL. An aliquot of the azide stock solution (100 μL) was added immediately before the start of kinetic runs. Volumes of water, phosphine, or azide used were adjusted accordingly in experiments where the concentrations of these reagents were varied.

NMR experiments designed to investigate the kinetic order of the Staudinger ligation with respect to phosphine, benzyl azide, and water were performed with either a Bruker DRX-500 spectrometer equipped with a 5 mm *z*-gradient broadband probe or a Bruker AV-400 spectrometer equipped with a 5 mm *z*-gradient broadband probe at ambient temperature (20 ± 0.5 °C), as verified by $\Delta\delta(CH_3\text{-}\delta OH)$ for a neat methanol sample. ^{31}P NMR spectra were obtained using a 90° pulse (6.1 μs) with a 60 s delay between scans to allow full relaxation (typical T_1 values for the various ^{31}P species were measured to be <10 s). One scan was acquired for each time point. The first scan was typically taken within 3 min after addition of the azide. All kinetics experiments were performed in triplicate.

^{31}P NMR spectra were processed using the Bruker XWinNMR software v3.5 with a line broadening of 2 Hz. Peak areas were integrated automatically and normalized to the triphenylphosphine oxide resonance. Data were plotted and analyzed using Microsoft Excel X.

Acknowledgment. We thank Dr. Fred Hollander for solving the crystal structure of intermediate **19**, and Dr. Ulla Andersen for mass spectrometry analyses. This work was supported by grants to C.R.B. from the National Institutes of Health (GM58867), and the Director, Office of Science, Office of Basic Energy Sciences, Division of Materials Science and Engineering and the Office of Energy Biosciences of the U.S. Department of Energy under Contract DE-AC03-76SF00098, and a grant to R.G.B. from the NSF (CHE_0345488).

Supporting Information Available: CIF data for compound **19**. This material is available free of charge via the Internet at http://pubs.acs.org.

JA044461M